# Effect of hygrothermal conditioning on the machining behavior of biocomposites

Faissal CHEGDANI[a] * and Mohamed EL MANSORI[a,b]

[a] *Arts et Métiers Institute of Technology, MSMP, HESAM University, F-51006 Châlons-en-Champagne, France;*
[b] *Texas A&M Engineering Experiment Station, College Station, TX 77843, USA.*

## Abstract

This work aims to study the cutting behavior of biocomposites under different controlled hygrothermal conditions. This investigation choice is motivated by the fact that natural plant fibers such as flax are characterized by their hydrophilicity which makes them able to absorb water from a humid environment. This absorption ability is intensified when increasing the conditioning temperature. The moisture diffusion process affects considerably the mechanical properties of the resulting composite, which causes many issues during the machining operations. In this paper, moisture diffusion, chip form, cutting and thrust forces, and scanning electron microscope (SEM) observations are considered to explore the cutting behavior of flax fiber reinforced polylactic acid (PLA) depending on the hygrothermal conditioning time. Results reveal that moisture content in the biocomposite is significantly influenced by the conditioning temperature and the fiber orientation. Moisture content and fiber orientation affect both the curling behavior of the removed chip as well as the tool/chip interaction in terms of friction. The machinability of flax fibers reinforced PLA biocomposites depending on hygrothermal conditioning time is then investigated using SEM analysis in addition to analytical modeling. An analysis of variance is used finally to quantify the observed results.

**Keywords**: Machining; Biocomposites; Moisture; Temperature.

* corresponding author: F. Chegdani
E-mail: faissal.chegdani@ensam.eu
ORCID: 0000-0002-7643-9701

## 1. Introduction

Natural fiber reinforced biocomposites are nowadays used in different industrial applications thanks to their different technical and ecological advantages [1–4]. Plant bast fibers such as flax, hemp, and jute are the most used natural fibers in the composite industry thanks to their higher mechanical performances [5]. The use of biocomposites currently relates to structural applications, especially in the automotive, motorsport, and marine industries due to the recent development of the manufacturing processes of these eco-friendly materials [6].

The industrial interest in biocomposites for structural applications requires the development and improvement of their finishing processes, such as machining, to correctly transform the biocomposite parts to their industrial functionality with optimal accuracy and mechanical performances. Many scientific works have then been carried out to examine the influence of the fiber type, the fibrous structure, and the process parameters on the machinability of biocomposites [7–9]. It has been shown that natural plant fibers are distinguished by a multiscale cellular structure (cellulose microfibrils embedded in natural amorphous polymers of hemicellulose, lignin, and pectin [10]) that complicates the cutting behavior of these fibers within the composite structure due to the highest resulting transverse elasticity [8]. Hence, a multiscale approach has been developed for the machinability analysis of biocomposites [11]. This approach aims to identify the pertinent scale for analyzing the machining of the biocomposite surfaces by considering the multiscale structure of the natural fibrous reinforcement.

The cellulosic structure of natural plant fibers induces an additional issue related to their hygrometric properties. Indeed, natural plant fibers are considered hydrophilic because of their ability to absorb water molecules from the external environment via their hydroxyl groups [12]. Several literature studies demonstrated that moisture absorption

leads to modifying the mechanical characteristics of biocomposites and this hygrometric impact has shown a scale effect. At a macroscopic scale, the moisture content seems to deteriorate the mechanical performances of biocomposites in terms of elastic tensile modulus, tensile strength, and bending modulus because of interface weakening, fiber plasticization, and polymer hydrolysis [13,14]. On the other hand, experimental investigations on isolated plant elementary fibers have highlighted that, in general, their mechanical properties show an increase when rising the water content [15,16]. This specific hygro-mechanical behavior has been explained by the fact that the water content contributes to a reorganization of cellulose microfibrils in the longitudinal direction of fibers, which increases consequently the mechanical properties by hygro-mechanical hardening.

The massive use of biocomposites in industrial applications requires mastering the whole manufacturing process chain, including the machining operations that are usually mandatory when finishing the composite parts with long natural fiber reinforcement in order to meet the standard accuracies and the requirements for assembly of the parts [7]. The machining of biocomposites shows significant challenges because of the complex structure of natural plant fibers [17]. Indeed, natural plant fibers are characterized by an important transverse elasticity due to their microstructure composed of different cellulosic cell walls [18]. Each cell wall contains cellulose microfibrils that are helicoidally structured in the longitudinal direction of fibers. Therefore, plant fibers show a high anisotropy, and the fiber orientation with respect to the cutting direction ($\theta$) must be considered to evaluate the machinability of the resulting biocomposite. The transverse elasticity of plant fibers causes defects in the machined surfaces such as uncut fiber extremities, especially when plant fibers are oriented with 90° regading the cutting direction because this orientation induces the highest transverse elasticity, while

biocomposites with fiber orientation of 45° show the lowest uncut fiber extremities since the direction of the shear force component is near that of the microfibrils [19].

Machining of biocomposites also shows significant sensitivity to the small variation of different material and/or process parameters such as the tool sharpness [20,21], the helix angle [22], the material temperature [23], the cutting speed and feed [24], and the depth of cut [25]. All these parameters affect the cutting contact stiffness that controls the involvement of shear, elastic deformation, plastic deformation, and friction mechanisms.

The complexity of a machinability analysis becomes more important for biocomposites when considering also the hygrometric effect. Indeed, the presence of moisture content due to exposure to a humid environment modifies the microstructure of plant fibers, which impacts the mechanical properties of the resulting biocomposites. This topic is not yet sufficiently addressed in the literature. However, the moisture aging effect has been previously considered by the authors to investigate the machining behavior of biocomposites made from flax fibers and polylactic acid (PLA) matrix using water immersion as a hygrometric conditioning process [26]. A specific effect of moisture content has been shown on the cutting behavior of the biocomposite at different hygrometric conditioning periods. Indeed, the moisture content improves the shearing mechanism of flax fibers at the microscale after a minimum hygrometric conditioning time required to change the cellulose microstructure. Nevertheless, this fiber shearing improvement does not imply a good surface finish at the meso- and macro-scale because water immersion contributes to interface damage due to the hydrolysis phenomenon, which induces debonding zones between fibers and matrix, leading to important subsurface degradation.

In this paper, the contribution of the conditioning temperature will be considered in addition to the hygrometry. This investigation choice is motivated by the important hygrothermal coupling effect that has been shown in a few literature studies on moisture diffusion and the mechanical behavior of biocomposites at different scales. Indeed, increasing the temperature of the hygrometric conditioning leads to an acceleration of the water diffusion into the biocomposite structure [27–29]. The hygrothermal impact on the mechanical performances of elementary flax fibers has been revealed in [30] where flax fibers without a humid environment show a significant decrease in their mechanical properties depending on temperature increase. However, the presence of a humid environment reduces the thermal effect on plant fibers. This can be explained by the fact that the moisture content in plant fibers contributes to an increase in their mechanical properties due to the rearrangement of cellulose microfibrils. The hygrometric hardening of flax fibers could offset the decrease of their mechanical properties due to the thermal softening of their natural polymeric components. It is important to note that the hygrothermal effect on biocomposites is highly related to other factors such as the matrix type (thermoplastic or thermoset) and the hygrometric conditioning process (total water immersion or exposure to relative humidity) [27–29]. Therefore, the hygrothermal aspect and its effect on biocomposites are highly important to consider for the industrial manufacturing of biocomposite parts in order to master and improve the technical functionalities of the final products. This consideration becomes imperative in the case of machining where the cutting contact interaction is mainly controlled by the mechanical properties of the work-material. As of today, the literature lacks scientific data concerning the cutting behavior of biocomposites under hygrothermal conditioning.

Hygrothermal conditioning (HTC) is performed in this study using a climatic chamber as it is the more realistic process to simulate the environmental conditions

(humidity and temperature). Cutting experiments are conducted on biocomposites made from flax fibers and PLA. Different fiber orientations with respect to the cutting feed and cutting length direction are considered to depict the effect of the natural reinforcement structure in the case of the machining of a unidirectional fabric. Machinability assessment regarding the HTC is carried out by capturing the microscopic state of machined surfaces, analyzing the chip morphology, and assessing the machining forces.

## 2. Materials and methods

Biocomposite samples are supplied from the "*Kaïros biocomposite*" group in France and are made of unidirectional flax fibers and PLA matrix as shown in Figure 1(a). The biocomposite plates are manufactured using a thermo-compression of 11 layers of thin films of PLA and 10 layers of unidirectional flax fabric at 200°C with a pressure of 1 bar for 5 min, followed by cooling with a pressure of 7 bars to reach 25°C in 5 min. This composition provides a fiber volume fraction of 23.7%. The received flax/PLA plates are cut into small rectangular samples with the dimensions of 30×20×3.5 $mm^3$. All samples have been subjected to polishing of their worksurfaces to ensure similar initial surface states.

As shown in Figure 1(b), flax fibers exhibit deferent forms, typically separated elementary fibers and small fiber bundles. Indeed, flax fiber extraction is in general carried out mechanically by scutching to separate the bundle from the rest of the stem [31]. Fiber bundles are then subjected to hackling to separate them into smaller bundles called technical fibers. Technical fibers are the conventional structure of plant fibers used in polymer composites. Each technical fiber is composed of a few elementary fibers gathered together via pectic interfaces [32]. It can be noticed from Figure 1(b) that elementary flax fibers show a significant variation in shape and diameter, which impacts

the size of technical fibers and their distribution as shown in Figure 1(c,d). Indeed, Figure 1(c) reveals a variation in the thickness of the flax fabrics.

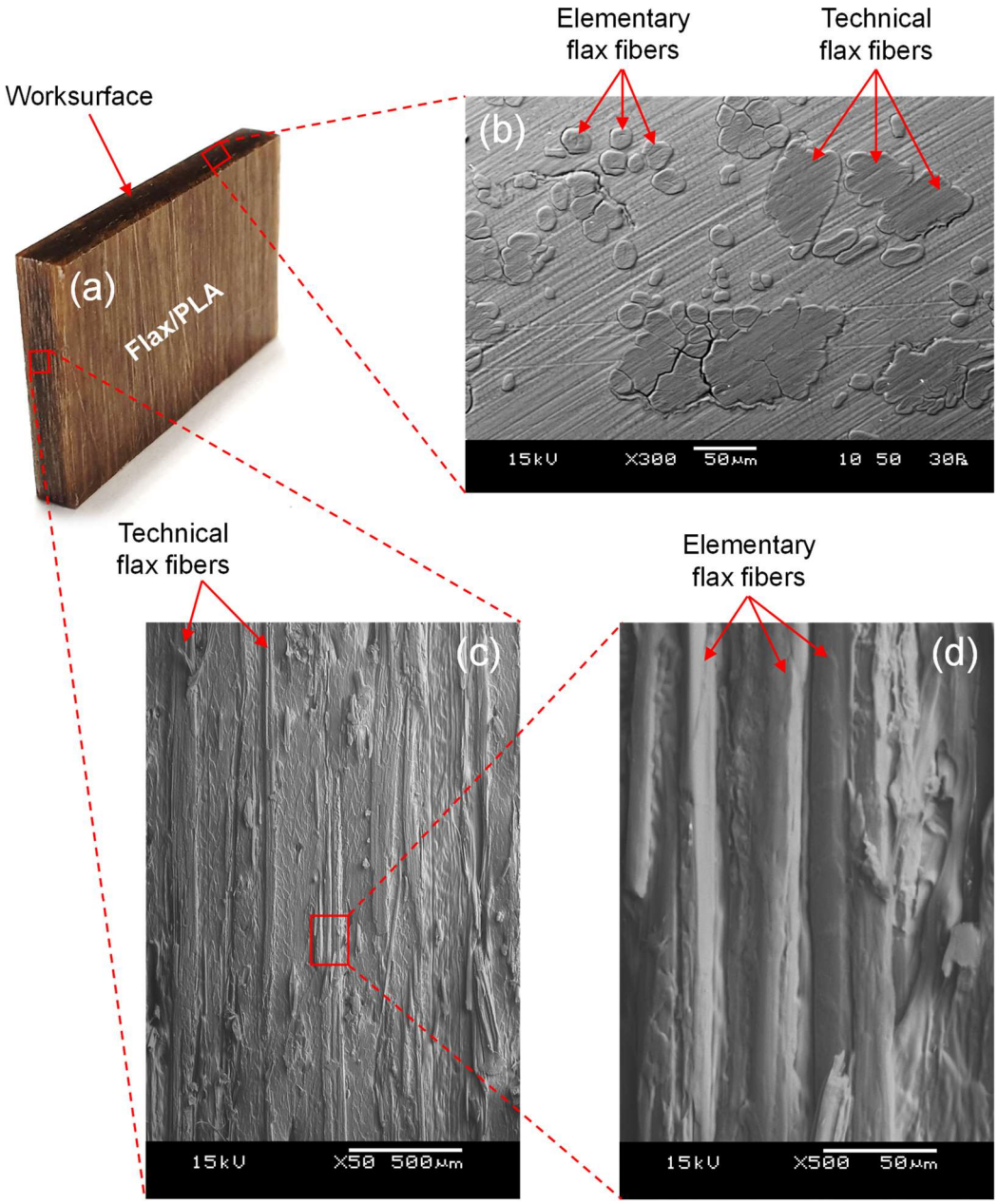


*Figure 1: (a) Photograph of the flax/PLA biocomposite sample, (b) SEM image of the flax/PLA worksurface before HTC conditioning and machining, (c,d) SEM section view of the biocomposite sample in the direction of the fibers*

Before performing the cutting experiments, biocomposite samples are conditioned in a climatic chamber (Figure 2(a)) at different conditioning durations that vary from 1 week to 5 weeks. The relative humidity is kept constant ($90^{\pm 3}$ %RH) while two conditioning temperatures are considered (30°C and 60°C). Reference conditioning

configurations are also investigated at each considered temperature where the biocomposite samples are subjected to only thermal conditioning on the climatic chamber for 24 hours at 30°C and 60°C.

The orthogonal cutting configuration has been considered in this investigation to overcome the effect of the tool trajectory in the other cutting processes and to get a fundamental understanding of the elementary mechanisms of the chip forming and surface generation depending on the hygrothermal conditions. Three values of fiber orientation (θ in Figure 2(b)) are used from 45° to 90°. A carbide cutting tool is used in the experiments and it is provided by "*Sandvik Coromant*" in France (ref. TCGX 16 T3 04 – AL H10). The cutting tool is characterized by a rake angle of $\gamma = 20°$ and a clearance angle of $\alpha = 7°$. Cutting experiments are carried out on a shaper machine (Model GSP – EL 136) that gives some predetermined values of the cutting speed to be selected by the user, from 8 m/min to 100 m/min. Increasing the cutting speed improves the machinability of biocomposites as shown in [33]. However, the cutting speed has been set at 50 m/min to avoid excessive vibration of the cutting setup. Cutting parameters are kept constant to focus only on the fiber orientation effect regarding the hygrothermal conditioning. Therefore, the depth of cut (ap) has been set at 100 µm according to the optimal cutting conditions obtained in [25,26]. A piezoelectric dynamometer (Model Kistler – 9255B) is considered to acquire the force signal data in the Cartesian coordinate system. As shown in Figure 2(c), data collection has been carried out with an amplifier (Model Kistler – 5017 B1310) connected to a data acquisition card (Model National Instruments – BNC-2110). Machining forces display is performed with a LabVIEW data recorder program at a sampling rate of 5000 Hz.

Each machining experiment has been repeated three times (at least) to check the repeatability of the measurements. The shapes of the formed chips are explored by

capturing an image of the removed chip of each cutting configuration using an optical microscope (Model Nikon – SMZ 745T). The machined surfaces of biocomposites are examined using a scanning electron microscope at low vacuum mode (Model JEOL – 5510LV).

For a better understanding of the effect of the HTC time, the fiber orientation, and the conditioning temperature on the hygrothermal properties and the machining behavior of flax fiber reinforced PLA biocomposites, an analysis of variance (ANOVA) has been carried out using a multilevel factorial design of experiments [34]. Based on the determination coefficient ($R^2$) of each ANOVA model, the contribution rate of each factor is calculated at $R^2$ confidence. More details about the used ANOVA in [35]. Table 1 gives the input factors for the experimental design.

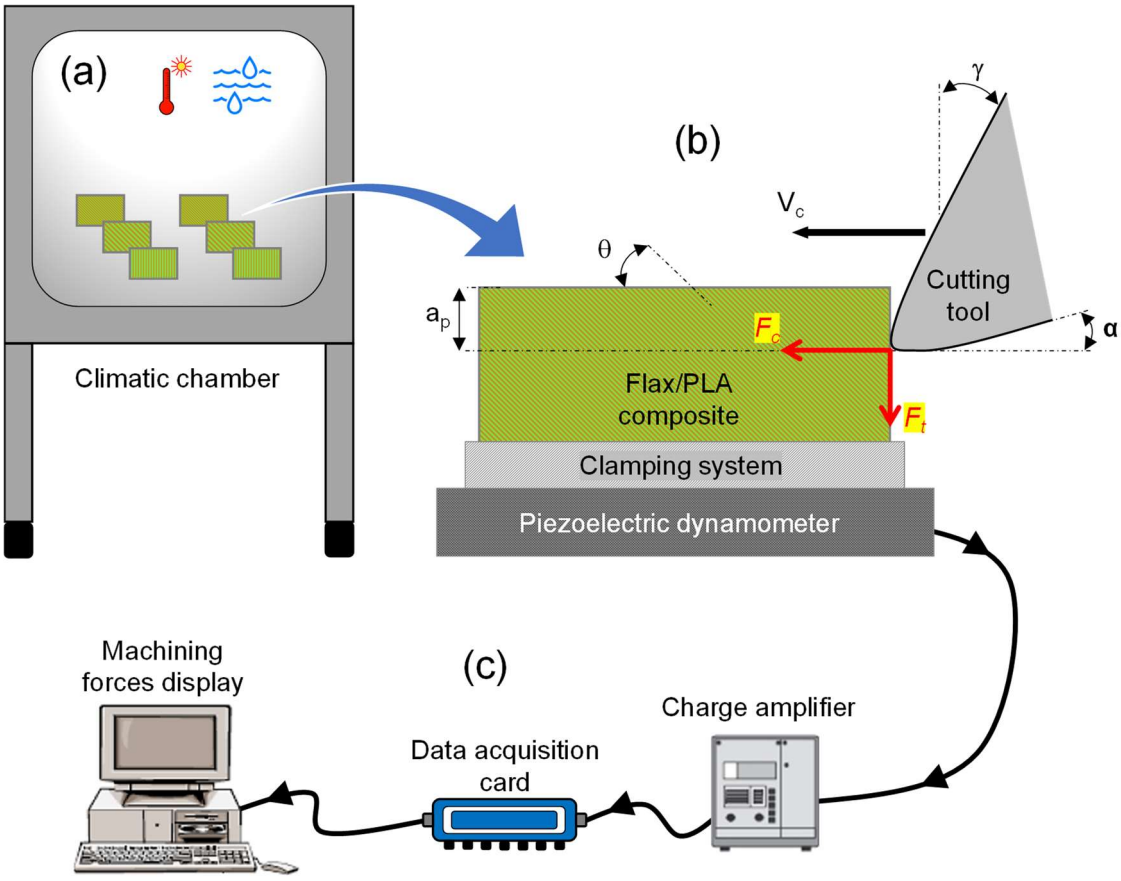


*Figure 2: Schematic illustration of the experimental setup for the orthogonal cutting of biocomposites with hygrothermal aging*

*Table 1: List of input parameters for the multilevel factorial design of experiments*

| Factor | Name | Unit | Levels |
|---|---|---|---|
| A | HTC time | Week | 0<br>1<br>2<br>3<br>4<br>5 |
| B | Fiber orientation | Degree (°) | 45<br>65<br>90 |
| C | Temperature | Degree C (°C) | 30<br>60 |

## 3. Results and discussion

### *3.1. Influence of hygrothermal conditioning on the moisture content*

Figure 3 shows the moisture content behavior in the biocomposite samples after each hygrothermal conditioning (HTC) configuration. The moisture content ($W_c(\%)$) is calculated using the following equation (1) where $M_i$ is the initial biocomposite mass and $M_f$ is the biocomposite mass after the HTC.

$$W_c = \frac{M_f - M_i}{M_i} \times 100 \qquad (1)$$

Figure 3 shows that increasing the conditioning temperature leads to the acceleration of the moisture diffusion in the biocomposite, which is in concordance with the literature results [27–29]. Depending on the conditioning temperature, the moisture content curves have different trends. For T=60°C, the water diffusion curves show an increase of the water content in relation to the HTC time until reaching a saturation from 3 weeks of HTC. When using T=30°C, the water diffusion curves do not show a stabilization after 5 weeks of HTC, which indicates that the water diffusion is still on the

transient regime and has not reached saturation yet. Hence, increasing the conditioning temperature leads to reaching the moisture content saturation more quickly.

Figure 3 reveals also that increasing the fiber orientation regarding the sample length from 45° to 90° contributes to the increase of both the water diffusion and the moisture content at saturation. Indeed, flax fibers are mainly responsible for moisture absorption and diffusion in the composite [27]. When increasing the fiber orientation regarding the sample length from 45° to 90°, flax fibers become shorter (orientation toward the sample width) and the diffusion becomes easier in the fiber length.

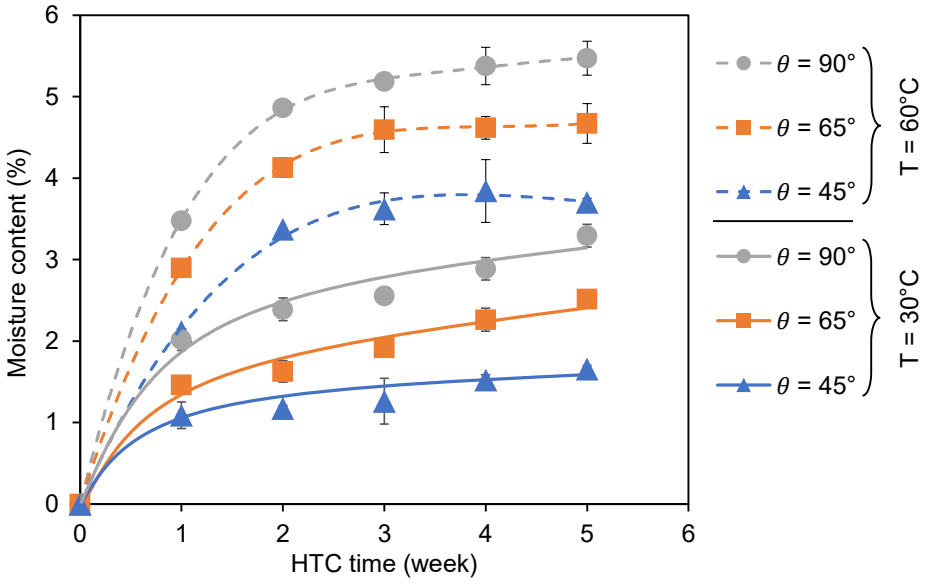


*Figure 3: Water content evolution of flax/PLA biocomposites depending on HTC temperature and fiber orientation*

### *3.2. Influence of hygrothermal conditioning on the machining forces*

Figure 4 presents the machining forces behavior, typically the cutting forces ($F_c$ in Figure 2(b)) and the thrust forces ($F_t$ in Figure 2(b)), depending on fiber orientation and HTC time. Cutting forces increase by increasing the fiber orientation, while the thrust forces show a decrease by increasing the fiber orientation. These results are in good agreement with the experimental observations in the machining of synthetic fiber composites [36–38].

Regarding the effect of HTC, Figure 4 shows that the behavior of the machining forces is modified when changing the conditioning temperature. At T=30°C, cutting and thrust forces decrease with the increase of the HTC time. However, cutting forces show a stabilization after 2 weeks of HTC (Figure 4(a)), while a re-increase of the thrust forces is revealed from 2 weeks of HTC (Figure 4(b)). This behavior of machining forces related to the HTC is similar to that observed with water immersion [26] since the conditioning temperature in water immersion (25°C) was near 30°C. The diminution in the cutting forces after introducing the HTC is attributed to water molecules that induce damage in the biocomposite interfaces, which contributes to reducing the mechanical strength of the biocomposite structure during the interaction with the cutting tool. On the other hand, the decrease in the thrust forces when starting the HTC is due to the plasticization mechanism of the amorphous components of the plant fiber. Then, the re-increase of the thrust forces in relation to the HTC time could be due to the re-increase of the fiber stiffness (and consequently their spring-back) after a certain conditioning time threshold (2 weeks in this study) because the water molecule leads to the reorganization of cellulose microfibrils in the longitudinal direction of fibers from a certain water content threshold as explained in the introduction.

At T=60°C, Figure 4(c) shows that increasing the conditioning temperature leads to a decrease in the cutting forces at the beginning of the HTC that can be attributed to the thermal softening of the polymeric component of the matrix and the natural fibers. However, the cutting forces increase depending on the HTC time until reaching the threshold of 2 weeks after which the cutting forces are stabilized (as for the conditioning temperature of 30°C). This behavior could be explained by the presence of the humid environment that reduces the thermal effect on plant fibers because the moisture content contributes to an increase in their mechanical properties due to a hygro-mechanical

hardening of flax fibers by the rearrangement of cellulose microfibrils as described in the introduction.

For the thrust forces at T=60°C, the behavior is similar to that with T=30°C at the beginning of the HTC until reaching the threshold of 2 weeks of HTC. After this specific conditioning duration, thrust forces show a stabilization rather than a re-increase. The fact that the thrust forces do not show a re-increase by hygro-mechanical hardening of flax fibers is probably caused by the thermal softening of the PLA matrix at this range of conditioning temperature. The thermal softening of the PLA matrix weakens the holding of flax fibers into the composite structure, which leads to lowering the normal reaction force of the biocomposite during the cutting operation.

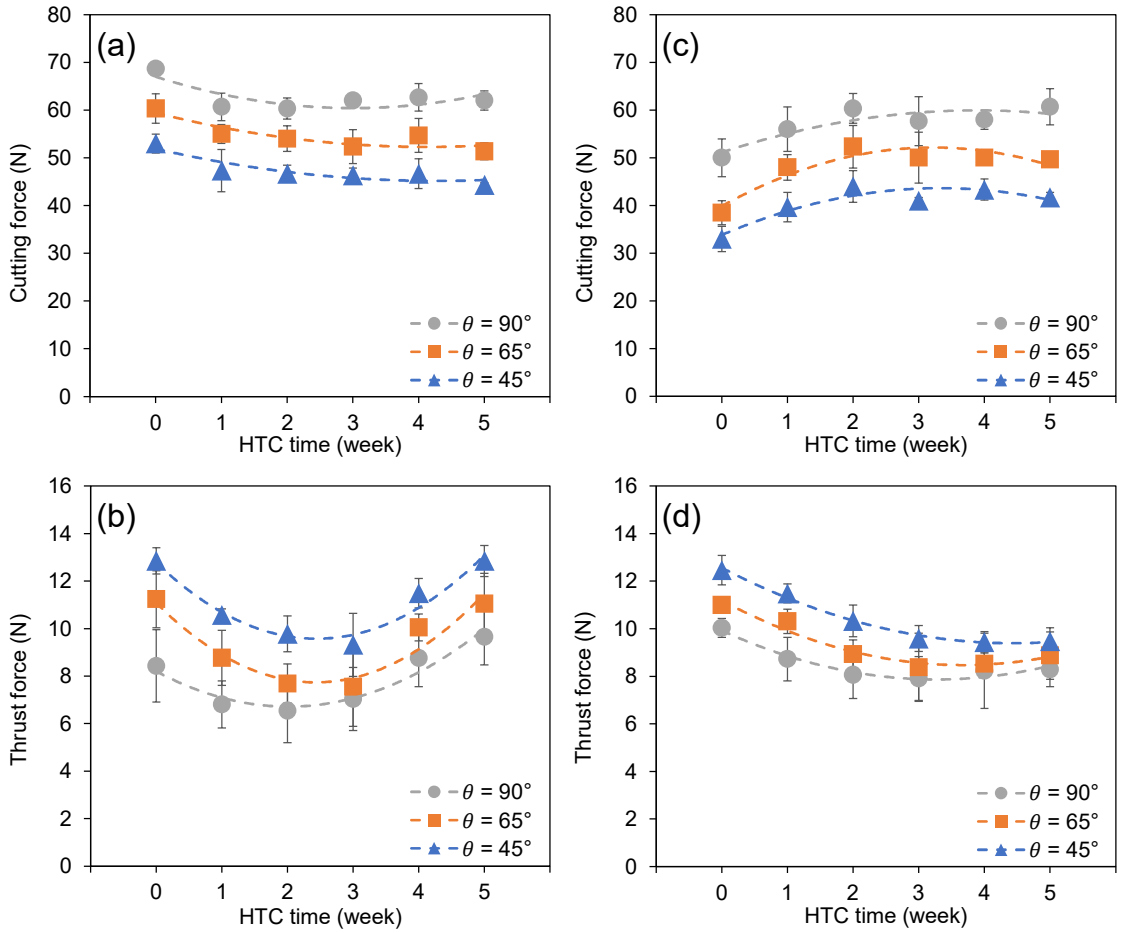


*Figure 4: Evolution of machining forces in orthogonal cutting of flax/PLA composites at different hygrothermal conditions. (a,b) at T=30°C, and (c,d) at T=60°C*

### *3.3. Hygrothermal effect on the chip formation*

#### *3.3.1. Hygrothermal effect on the chip curling*

Figure 5 gives the shape of the formed chips at different cutting and hygrothermal conditions. All the considered conditions show a continuous chip that is characteristic of biocomposites with a thermoplastic matrix [23]. With a fiber orientation of 45°, no significant effect of the HTC on the chip formation can be noticed. However, when increasing the fiber orientation from 45° to 90°, the HTC becomes strongly significant on the chip forming where the chips show high curling at θ=90° by introducing the HTC. The chip formation process of biocomposites with $\theta = 90°$ corresponds to the experimental observations of [26].

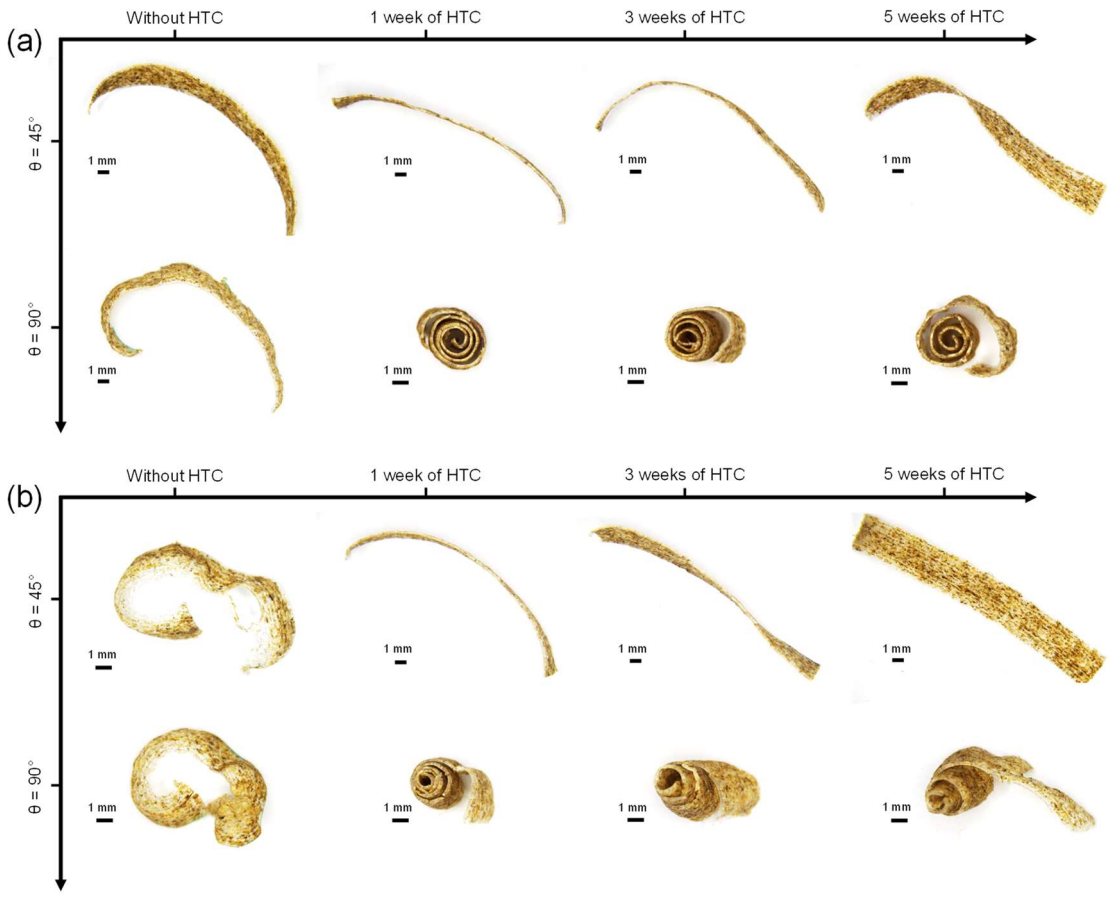


*Figure 5: Shape of the formed flax/PLA chips under hygrothermal conditioning at (a) T=30°C and (b) T=60°C*

The chip curling is mainly controlled by the bending moment required to modify the chip curvature radius. This specific bending moment is proportional to the flow stress during the tool-material interaction [39,40]. Indeed, the bending moment ($M_{fp}$) is given by the equation (2) where $\sigma_0$ is the flow stress, $b$ is the chip width, and $t_c$ is the chip thickness.

$$M_{fp} = \frac{\sigma_0 \, b \, t_c^2}{4} \qquad (2)$$

With θ = 90°, the transverse mechanical properties of biocomposites (modulus and strength) show a significant decrease at the beginning of the HTC and then a stabilization [41]. This could explain the curling of the removed chip with HTC at θ = 90° because of the reduction of the required bending moment that may be attributed to the decrease of the transverse mechanical properties. When increasing the conditioning temperature at θ = 90°, Figure 5(b) shows oblique curling that could be attributed to the highest moisture content at this range of temperature, which can induce a self-shaping in the oblique direction due to moisture-induced bending actuation described in [42,43].

With θ = 45°, fibers are oriented near the shearing force direction as shown in [19]. The flow stress of the tool/material interaction should be the highest because the main mechanical properties of fibers are toward their longitudinal direction. This means that the bending moment required to modify the chip curvature radius is the highest, which participates in preventing the chip from curling. The chip with θ = 45° is formed with a succession of interlaminar shear that is not controlled by the moisture absorption in flax fibers.

Without HTC, Figure 5(b) shows that increasing the conditioning temperature contributes to an increase in the chip curling. This behavior could be attributed to the thermal softening of the polymer that leads to a decrease in its flow stress and, as a

consequence, a decrease in the required bending moment. Indeed, the glass transition temperature ($T_g$) of the PLA matrix is around 55°C [44]. On the other hand, flax fibers without controlled humidity show an important decrease in their mechanical properties depending on temperature increase until reaching 60°C [30]. Then, introducing humidity reduces the thermal effect on flax fibers as shown in [30].

### *3.3.2. Hygrothermal effect on the tool/chip interaction*

The tool/chip interaction is investigated in this paper by calculating the tool/chip friction coefficient from the machining forces using the Merchant model that has been validated for use in the machining analysis of biocomposites [19]. The coefficient of friction (COF) at the tool/chip interface can be calculated using equation (3) where Fc, Ft, and γ are respectively the cutting force, the thrust force, and the rake angle (see Figure 2).

$$COF = \frac{F_t + F_c \tan(\gamma)}{F_c - F_t \tan(\gamma)} \quad (3)$$

Figure 6 presents the results of the COF for all the considered cutting conditions. In general, the increase of the fiber orientation from 45° to 90° contributes to a decrease in the COF. Without HTC, increasing the temperature leads to an increase in the COF at the tool/chip interface, which is attributed to the increase of both the contact area and the work of adhesion [45]. By increasing the HTC time, the behavior of the COF at the tool/chip interface is different depending on the conditioning temperature. Indeed, Figure 6(a) shows an increase in the COF regarding the HTC time at T=30°C, while Figure 6(b) reveals a decrease in the COF regarding the HTC time at T=60°C.

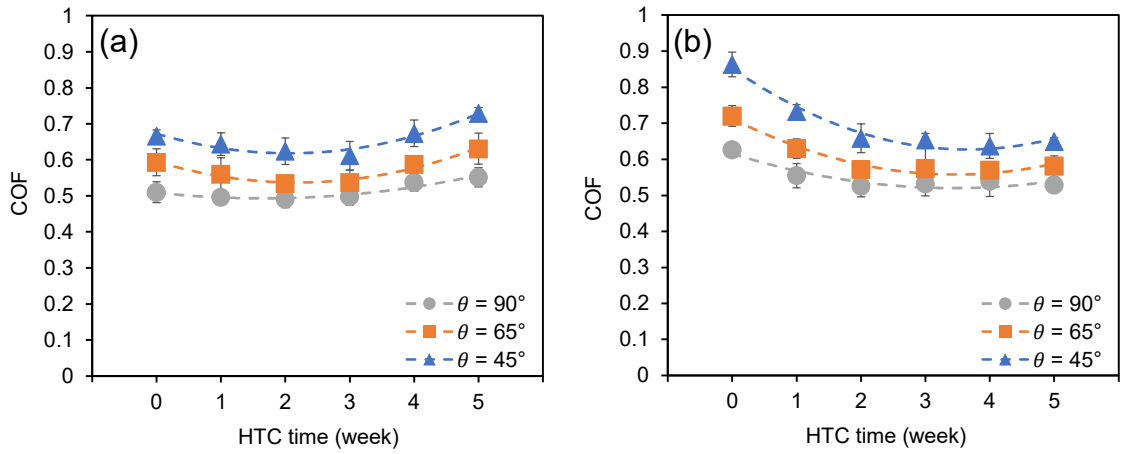


*Figure 6: Evolution of the tool/chip COF at the different cutting conditions for (a) T=30°C and (b) T=60°C*

Understanding the COF behavior depending on the HTC time requires the identification of the elements involved at the tool/chip interface. In order to do so, Figure 7 and Figure 8 present micrographic observations of the chip surfaces from the tool/chip interface at 30°C and 60°C respectively. At T=30°C the microscopic images of Figure 7(a,c) without HTC show a high rate of deformed fibers on the chip from the tool/chip interface, in addition to a plastic flow of the PLA matrix due to its deformation during machining. The rate of deformed fibers on the tool/chip interface seems to be slightly higher in the case of θ=90°. This can be explained by the fact that the fibers with θ=45° generate less deformation because they are on the cutting shear plan as shown in section 3.3.1. By moving forward to 5 weeks of HTC, Figure 7(b,d) show an intensification of the matrix flow instead of fiber deformation, especially for θ=45°.

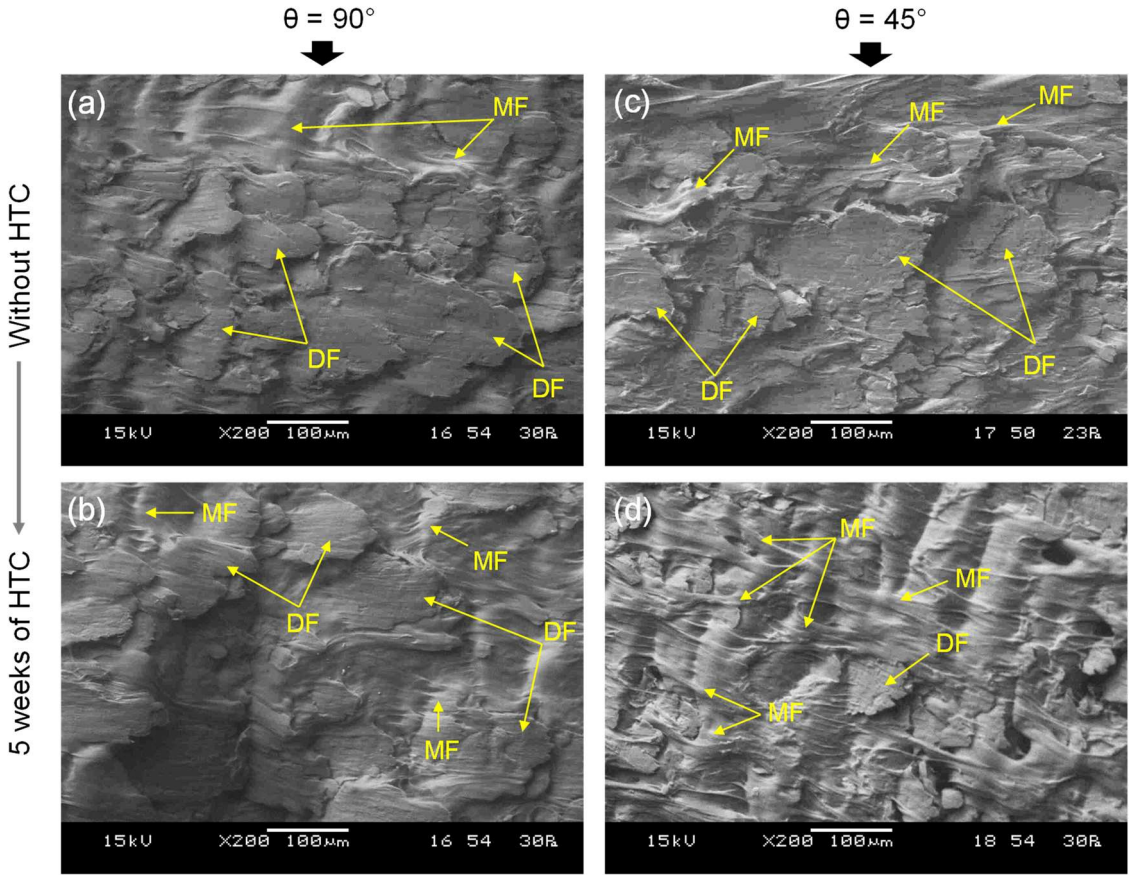


*Figure 7: SEM images of chip surfaces from the tool/chip interface at T = 30°C. DF: deformed fibers, MF: matrix flow*

In the case of T=60°C, Figure 8(a,c) show more plastic flow of the PLA matrix without HTC compared to the samples conditioned at 30°C in Figure 7(a,c). This behavior is probably induced by the thermal softening of the PLA matrix at this range of temperature which increases its plastic deformation. At 5 weeks of HTC, Figure 8(b,d) reveal that the matrix flow is reduced to the detriment of more deformed fibers. The fibers are more deformed in the case of θ = 90° where the presence of uncut fiber extremities as shown in Figure 8(b) can be also noticed.

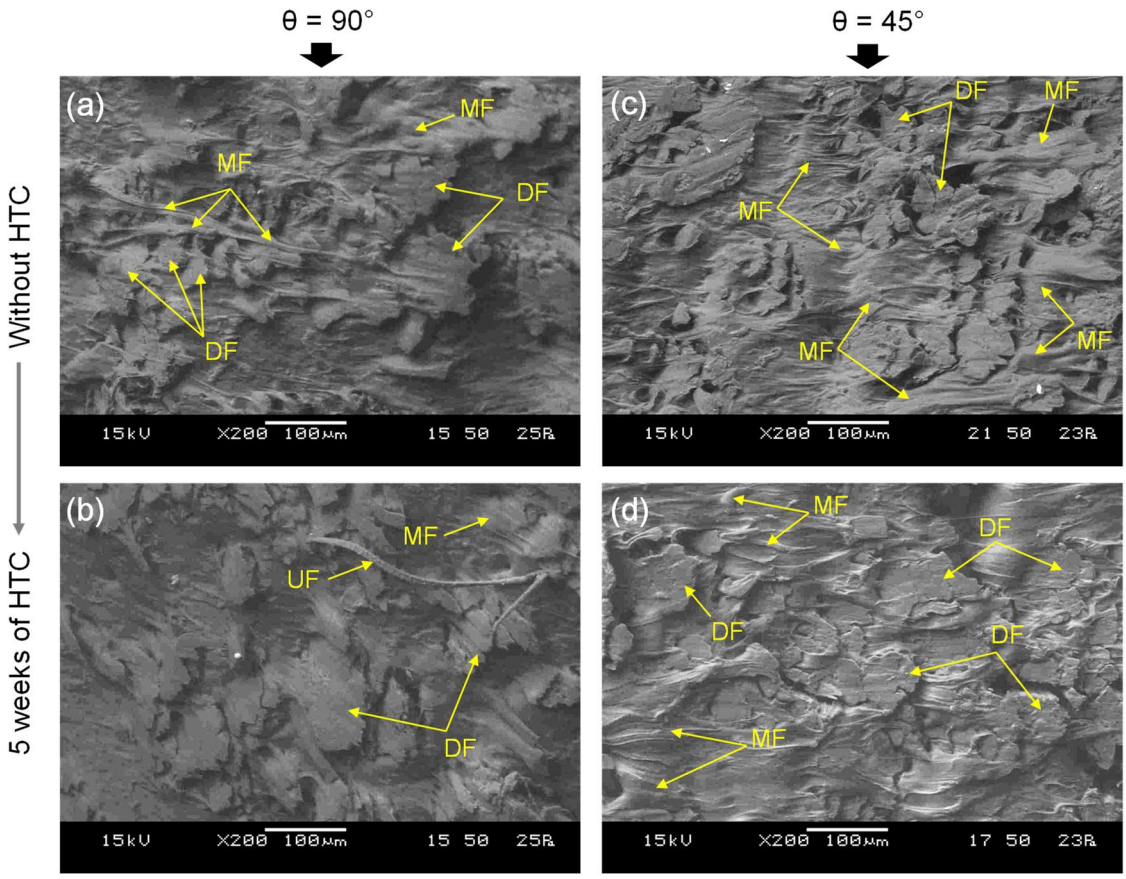


*Figure 8: SEM images of chip surfaces from the tool/chip interface at T = 60°C. DF: deformed fibers, MF: matrix flow, UF: uncut fibers*

The SEM analysis in Figure 7 and Figure 8 can explain the COF behavior revealed in Figure 6 through the non-abrasive power of natural plant fibers that can act as a third body lubricant as shown in [46–48]. Indeed, the presence of a high rate of fiber extremities at the tool/chip interface (Figure 7(a,c) and Figure 8(b,d)) contributes to reducing friction. However, the increase of the matrix flow (Figure 7(b,d) and Figure 8(a,c)) makes more contact with the polymer matrix than with flax fibers, which leads to an increase in the COF. Similarly, the SEM images with $\theta = 90°$ show a higher rate of uncut fiber extremities on the chip surface than that of $\theta = 45°$, which can also explain the lowest COF values for $\theta = 90°$.

### *3.4. Hygrothermal effect on the cutting behavior of the biocomposite*

Figure 9 shows the machined surfaces with $\theta = 45°$ depending on the different hygrothermal conditions. At 30°C, increasing the HTC time leads to an improvement in the cutting efficiency of flax fibers since the shape of elementary fibers starts to be clearly visible after 5 weeks of HTC as shown in Figure 9(c). However, some decohesion zones are noticeable after HTC (Figure 9(b,c)) which is due to the failure of the interfaces. At 60°C, the cross-sections of elementary fibers after HTC ((Figure 9(e,f)) do not present a neat cut as for the cutting at 30°C, indicating a deformation of fibers toward the cutting direction and, consequently, a reduction of the shearing efficiency.

The machined surfaces with $\theta = 90°$ depending on the different hygrothermal conditions are presented in Figure 10. Without HTC, flax fibers are not efficiently sheared because Figure 10(a) shows a transverse deformation of the fibers' cross-sections toward the cutting direction. The increase in the temperature contributes to inducing more deformed fibers in addition to some uncut fiber extremities as shown in Figure 10(d). The observed cutting behavior of flax fibers is related to the decrease of their mechanical performances in terms of stiffness and strength by the increase in temperature [30], which leads to significant deformation of flax fibers before shearing. The viscoelastic comportment of flax fibers and PLA increases the ability of each biocomposite phase to deform when rising the temperature because of softness, high elasticity, and adhesion [23].

By introducing the HTC, it can be noticed an enhancement in the shear process of flax fibers at 30°C and 60°C as shown respectively in Figure 10(b) and Figure 10(e). At 3 weeks of HTC, the machined surface at 30°C exhibits an efficient shearing of fibers during cutting since the polygonal cross-sections of flax fibers are well-formed without any significant sign of damage or deformation. Indeed, the introduction of a certain water

content threshold inside the cell walls of plant fibers generates the mobility of microfibrils in the longitudinal direction of elementary fibers, which contributes to an increase in their mechanical properties in terms of rigidity and strength [49]. This could explain the improvement of the fiber cutting from 3 weeks of HTC at 30°C. However, the machined surfaces at 60°C after 3 weeks of HTC reveal a high rate of deformed fibers and a poor shearing efficiency. This could be attributed to the thermal softening of the PLA matrix that prevents an efficient upholding of the fibrous reinforcement during the cutting process.

Figure 10 reveals also some damage in the interfaces caused by HTC time, especially at 30°C as observed in Figure 10(b,c). This interface damage leads to a decrease in the shear efficiency of flax fibers after 5 weeks of HTC as shown in Figure 10(c) where the cross-sections of flax fibers are no longer visible in the SEM images. Nevertheless, it can be noticed in Figure 10(e,f) that increasing the conditioning temperature contributes to reducing the debonding zones, which may be due to the increase of the thermomechanical plastic flow of the polymer matrix toward the cutting direction.

It is important to note that flax fibers oriented with $\theta = 45°$ are less affected by the HTC than those oriented with $\theta = 90°$. This is due to the fact that biocomposite samples with $\theta = 45°$ generate the lowest moisture content as shown in Figure 3. Moreover, flax fibers with $\theta = 45°$ are oriented near the shear plan (i.e. the shear force) which leads to an increase in the cutting efficiency of flax fibers at this orientation as shown in [19].

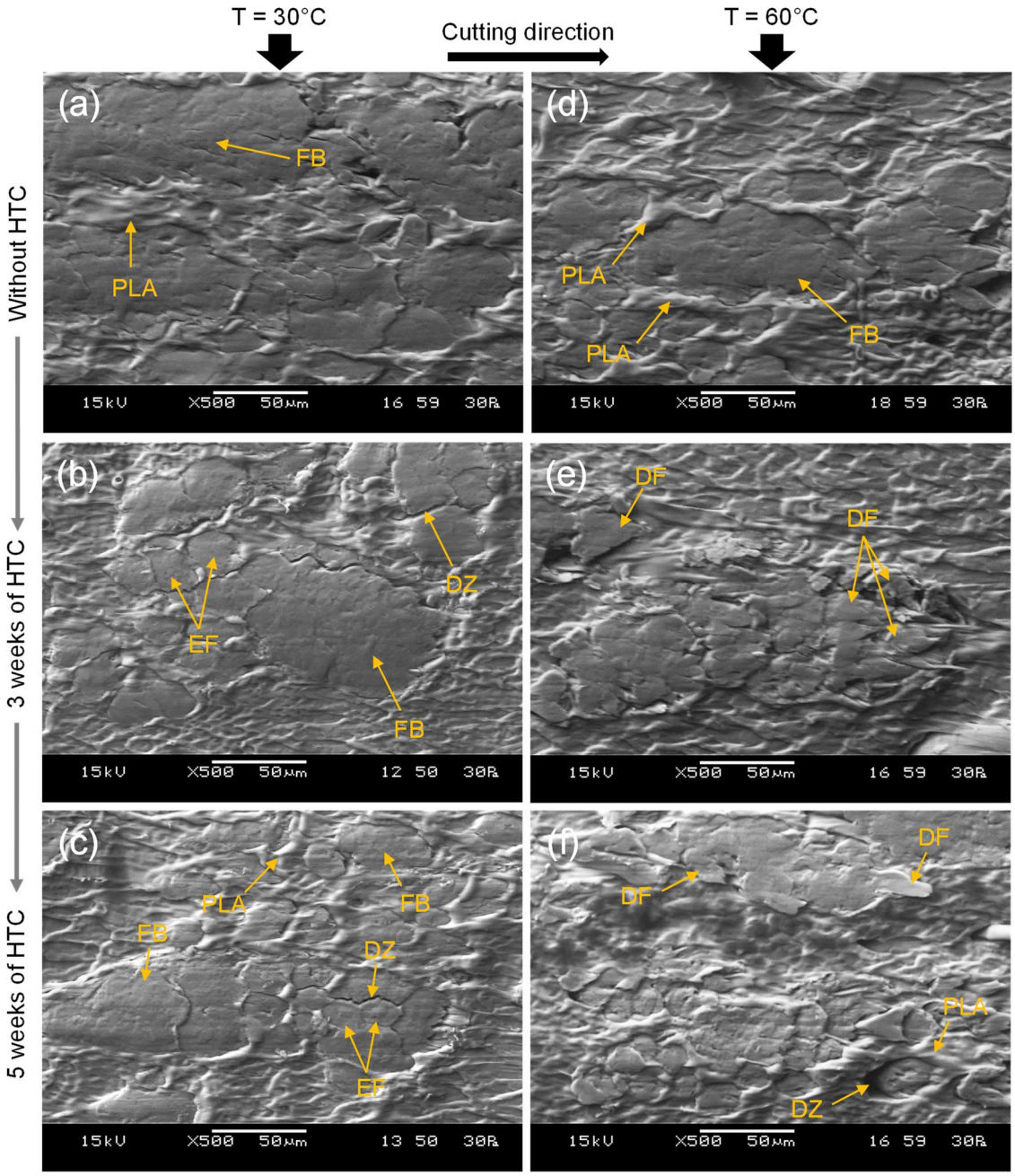


*Figure 9: SEM micrographs of machined surfaces with $\theta = 45°$ at different hygrothermal conditions. FB: fiber bundle, EF: elementary fibers, DF: deformed fibers, DZ: debonding zone*

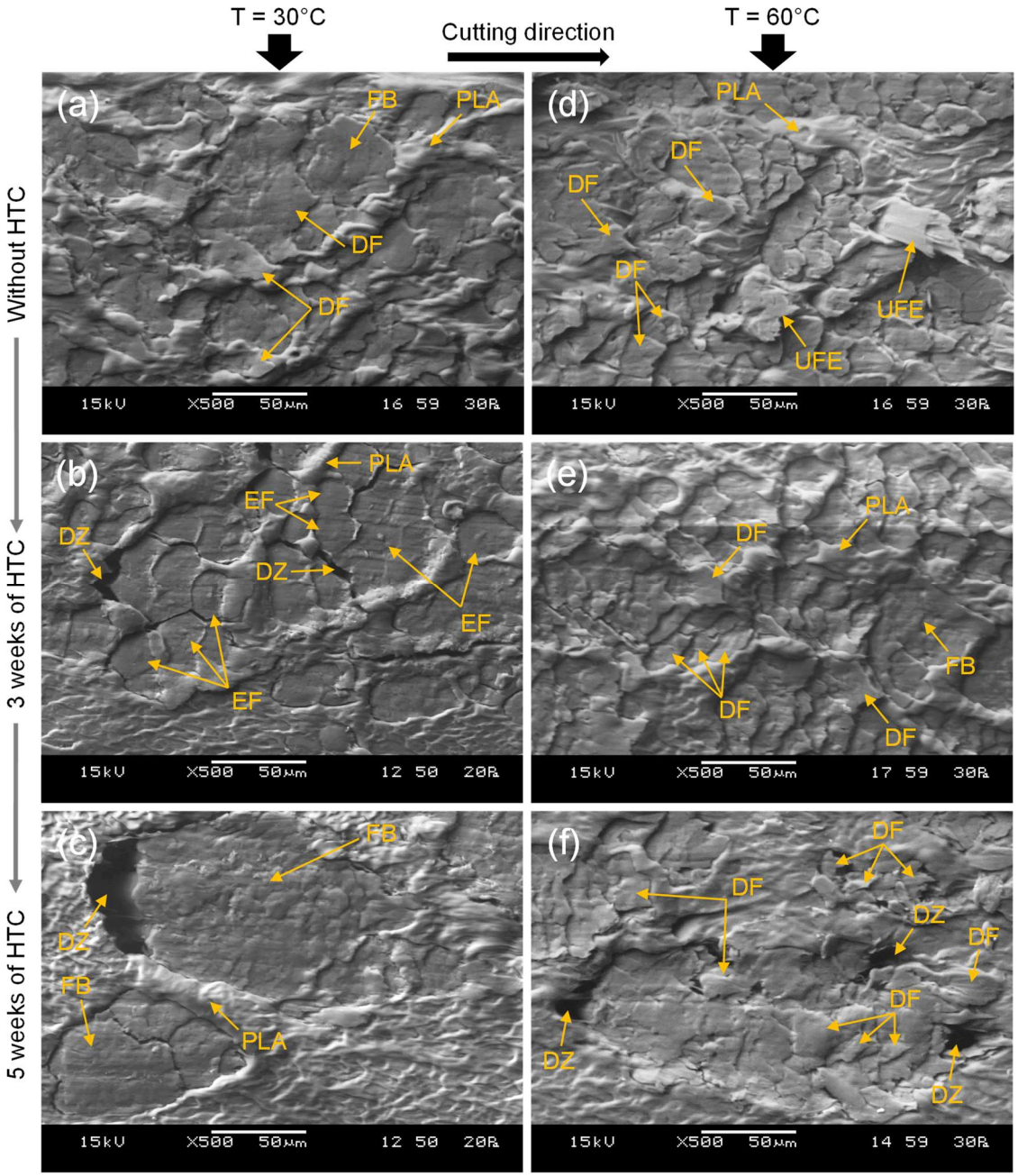


*Figure 10: SEM micrographs of machined surfaces with $\theta = 90°$ at different hygrothermal conditions. FB: fiber bundle, EF: elementary fibers, DF: deformed fibers, DZ: debonding zone, UFE: uncut fiber extremities*

For more understanding of the cutting mechanisms depending on the fiber orientation and the hygrothermal conditions, the analytical cutting model of Merchant [50] has been used to distinguish the contribution of shear and friction mechanisms to the machinability of the biocomposite. As shown in Figure 11, the machining behavior in the case of orthogonal cutting configuration is governed by material deformation on the primary shear zone, and tool/chip friction on the secondary shear zone. Based on the

Merchant model, the machining forces ($F_c$ and $F_t$ in Figure 11) recorded with the piezoelectric dynamometer can be decomposed to a shear force ($F_s$ in Figure 11) in the primary shear zone and a friction force ($F_f$ in Figure 11) in the secondary shear zone. $F_f$ and $F_s$ can be calculated following the equations (4) and (5) where $\gamma$ is the rake angle and $\phi$ is the shear angle.

$$F_f = F_c \sin\gamma + F_t \cos\gamma \quad (4)$$

$$F_s = F_c \cos\phi - F_t \sin\phi \quad (5)$$

The shear angle can be determined using equation (6) where "*c*" is the chip thickness ratio. Based on the Merchant assumptions, the chip thickness ratio is equivalent to the chip length ratio since the amount of side flow that occurs in the chip during removal is neglected [50]. This assumption has been validated previously in [19] for biocomposite cutting.

$$\tan\phi = \frac{c\cos\gamma}{1 - c\,\mathrm{si}} \quad (6)$$

Therefore, "*c*" can be determined using equation (7) where $L_2$ is the chip length, and $L_1$ is the initial cutting length.

$$c = \frac{L_2}{L_1} \quad (7)$$

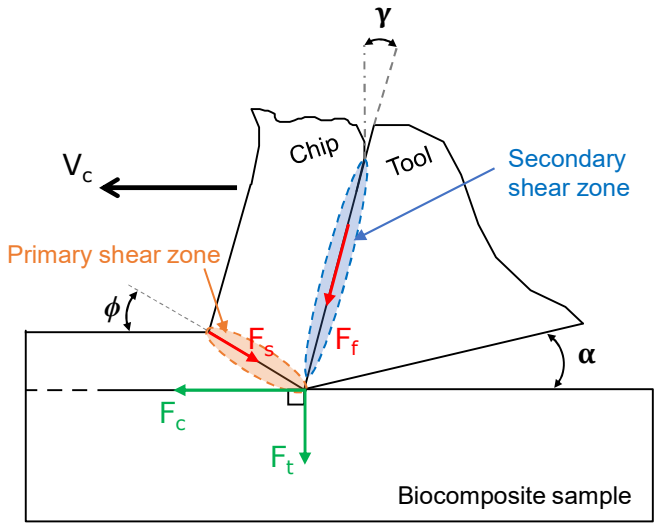


*Figure 11: Schematic illustration of the orthogonal cutting configuration showing the primary and the secondary shear zones*

Figure 12 shows the effect of fiber orientation and hygrothermal conditioning on the cutting shear angle. In general, increasing the fiber orientation leads to an increase in the shear angle. However, the effect of fiber orientation on the shear angle is insignificant without HTC. Moreover, the increase in the conditioning temperature decreases the shear angle and contributes to reducing the effect of the fiber orientation on the shear angle as shown in Figure 12(b). In the fundamentals of cutting, a small shear angle means a large shear plane and, consequently, a high material strain during the cutting operation [51]. Therefore, the results of Figure 12 are in good agreement with the microscopic observations of the chip surfaces because the SEM image of the chip surface with θ=45° under hygrothermal conditioning shows a high rate of matrix flow (see Figure 7(d)), which is a sign of a large material strain and a smaller shear angle. Moreover, introducing moisture content to the biocomposite at θ=45° contributes to a significant intensification of the plastic flow of the matrix as shown in Figure 7(c → d), which results in a sharp drop in the shear angle as shown in Figure 12(a).

When increasing the conditioning temperature, the polymer matrix is subjected to a thermal softening. This behavior leads to both an increase in the plastic strain of the

polymer and an increase in the transverse deformation of flax fibers due to the reduction of the polymer stiffness. All these mechanisms contribute to the increase of the biocomposite strain during cutting, which decreases the cutting shear angle and makes it less dependent on the fiber orientation.

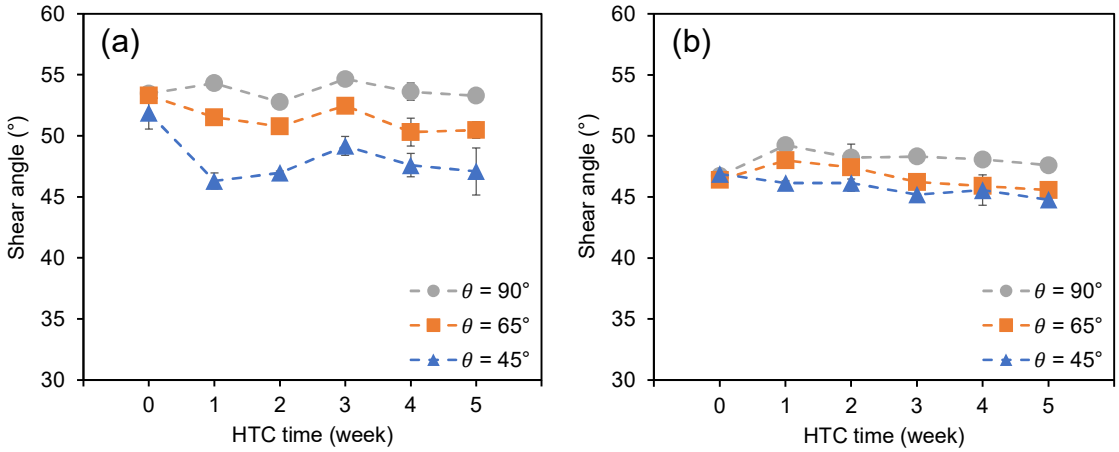


*Figure 12: Evolution of the cutting shear angle depending on the fiber orientation and the hygrothermal conditioning. (a) T=30°C, and (b) T=60°C.*

Figure 13 presents the results of the calculated shear forces and friction forces following the Merchant cutting model. It can be seen that the increase of the fiber orientation from 45° to 90° increases both the shear force and the friction force. However, the fiber orientation effect is more noticed in the shear forces (Figure 13(a,c)). Regarding the effect of the hygrothermal conditioning, it can be noticed a slight decrease of both shear and friction forces depending on the HTC time at T=30°C. When increasing the conditioning temperature to 60°C, the HTC does not have an important effect on the friction force (Figure 13(d), while the shear force shows a significant dependence on the HTC time (Figure 13(c)). Indeed, the shear force behavior at high conditioning temperature is similar to the moisture content behavior shown in Figure 3 where the shear force increases with the HTC time until reaching the saturation from 2 weeks of HTC.

By comparing the shear forces with the friction forces at different cutting conditions, it can be found that the shear force is higher than the friction force for θ=45°.

Then, the friction forces become higher than the shear forces when increasing the fiber orientation up to θ=90°. it can be concluded from these results that the increase of the fiber orientation from 45° to 90° leads to changing the predominant mechanism from friction to shear, which is in good agreement with the analysis of chip formation in section 3.3.2.

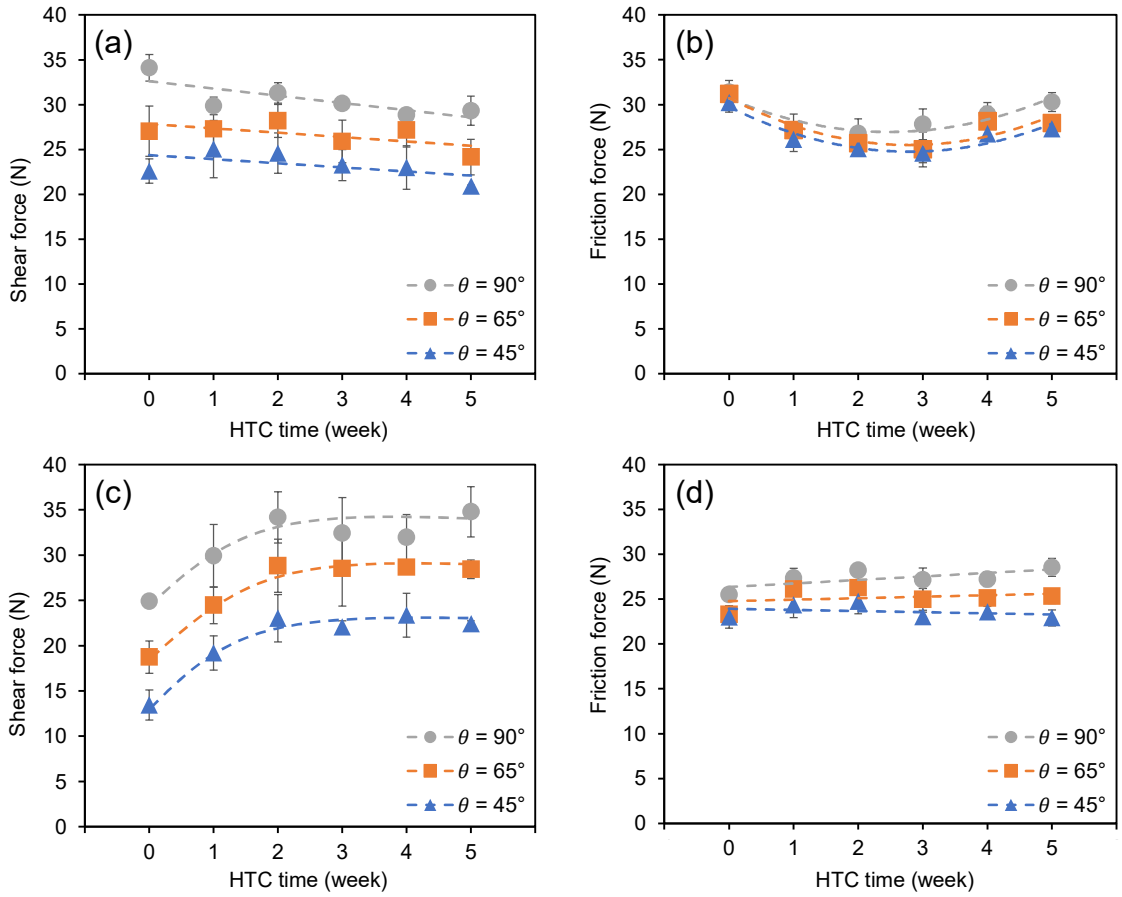


*Figure 13: Evolution of the shear force and the friction force depending on the fiber orientation and the hygrothermal conditioning. (a,b) T=30°C, and (c,d) T=60°C*

### *3.5. Quantification of the hygrothermal effect with ANOVA*

Statistical analysis of variance has been performed with a multilevel factorial experimental plan that includes the input factors of Table 1 to explain their effect on three output parameters: moisture content, cutting force, and thrust force.

Table 2 presents the results of ANOVA for the effect on the moisture content. All the main factors are significant since their increase leads to a rise in the moisture content in the composite. In addition, the interactions HTC time/fiber orientation and HTC time/temperature are also revealed significant in the ANOVA for the effect on moisture content. As explained previously, there is a significant interaction between the HTC time and the conditioning temperature regarding the effect on the moisture content since the increase of the temperature contributes to accelerating the moisture diffusion into the biocomposite.

*Table 2: ANOVA for the effect of input parameters on moisture content*

| Source | SS | DF | MS | F-value | p-value | Significance |
|---|---|---|---|---|---|---|
| **Model ($R^2$ = 0.99)** | 301 | 35 | 8.6 | 239.02 | < 0.0001 | significant |
| A-HTC time | 161.1 | 5 | 32.22 | 895.49 | < 0.0001 | significant |
| B-Fiber orientation | 25.05 | 2 | 12.52 | 348.04 | < 0.0001 | significant |
| C-Temperature | 87.04 | 1 | 87.04 | 2419.14 | < 0.0001 | significant |
| AB | 5.56 | 10 | 0.5559 | 15.45 | < 0.0001 | significant |
| AC | 21.87 | 5 | 4.37 | 121.57 | < 0.0001 | significant |
| BC | 0.2526 | 2 | 0.1263 | 3.51 | 0.0351 | |
| ABC | 0.1356 | 10 | 0.0136 | 0.3768 | 0.9529 | |
| **Pure Error** | 2.59 | 72 | 0.036 | | | |
| **Cor Total** | 303.6 | 107 | | | | |

*SS: sum of squares, DF: degrees of freedom, MS: mean square, Cor Total: corrected total sum of squares*

Table 3 presents the results of ANOVA for the effect on cutting force. Only the fiber orientation and the temperature are significant as the main factors. Indeed, the fiber orientation controls the mechanical properties of the biocomposite during the cutting

contact interaction, while increasing the temperature leads to thermal softening of the polymeric components of the composite which reduces the mechanical strength of the work-material during machining. The ANOVA of Table 3 also reveals a significant interaction between the HTC time and the temperature. This confirms the fact that the increase of the conditioning temperature, associated with a long HTC time, contributes to introducing damage to the composite, which affects the reaction contact force of cutting.

*Table 3: ANOVA for the effect of input parameters on cutting forces*

| Source | SS | DF | MS | F-value | p-value | Significance |
|---|---|---|---|---|---|---|
| **Model ($R^2$ = 0.86)** | 6969 | 35 | 199.11 | 12.79 | < 0.0001 | significant |
| A-HTC time | 71.33 | 5 | 14.27 | 0.9166 | 0.4753 | |
| B-Fiber orientation | 4616.17 | 2 | 2308.08 | 148.29 | < 0.0001 | significant |
| C-Temperature | 1095.7 | 1 | 1095.7 | 70.4 | < 0.0001 | significant |
| AB | 45.17 | 10 | 4.52 | 0.2902 | 0.9814 | |
| AC | 1109.07 | 5 | 221.81 | 14.25 | < 0.0001 | significant |
| BC | 8.46 | 2 | 4.23 | 0.2719 | 0.7627 | |
| ABC | 23.09 | 10 | 2.31 | 0.1484 | 0.9988 | |
| **Pure Error** | 1120.67 | 72 | 15.56 | | | |
| **Cor Total** | 8089.67 | 107 | | | | |

*SS: sum of squares, DF: degrees of freedom, MS: mean square, Cor Total: corrected total sum of squares*

Table 4 presents the results of ANOVA for the effect on thrust forces. The conditioning temperature is revealed as not significant on the thrust force compared to the other factors. The thermal softening of the polymeric components of the biocomposite, typically the PLA matrix, affects the machining behavior more in the feed direction (where the transverse properties of the composite are highly solicited) than in the normal direction. However, the conditioning temperature becomes significant when associated with the HTC time because it allows to increase meaningfully the moisture content which modifies the stiffness of flax fibers and leads to an intensification of the fiber spring-back when machining.

*Table 4: ANOVA for the effect of input parameters on thrust forces*

| Source | SS | DF | MS | F-value | p-value | Significance |
|---|---|---|---|---|---|---|
| **Model ($R^2$ = 0.71)** | 277.82 | 35 | 7.94 | 5.11 | < 0.0001 | significant |
| A-HTC time | 87.84 | 5 | 17.57 | 11.31 | < 0.0001 | significant |
| B-Fiber orientation | 121.97 | 2 | 60.98 | 39.25 | < 0.0001 | significant |
| C-Temperature | 0.0144 | 1 | 0.0144 | 0.0093 | 0.9235 | |
| AB | 7.81 | 10 | 0.7815 | 0.503 | 0.8825 | |
| AC | 49.82 | 5 | 9.96 | 6.41 | < 0.0001 | significant |
| BC | 8.16 | 2 | 4.08 | 2.63 | 0.0792 | |
| ABC | 2.19 | 10 | 0.2188 | 0.1408 | 0.999 | |
| **Pure Error** | 111.86 | 72 | 1.55 | | | |
| **Cor Total** | 389.68 | 107 | | | | |

*SS: sum of squares, DF: degrees of freedom, MS: mean square, Cor Total: corrected total sum of squares*

From the ANOVA results, the contribution rate (C (%)) of each factor is calculated and presented in Figure 14 for the moisture content and the two machining force components. The moisture content is strongly affected by the conditioning temperature (63 %), followed by the conditioning time (23%). These two significant factors control the kinematics of water diffusion in the composite. For the machining forces, both are highly impacted by the fiber orientation (54% for the cutting force and 46% for the thrust force) because the fiber orientation defines the structural cutting configuration of the composite in the case of unidirectional fabric. However, the cutting force is significantly influenced by the temperature (26%) due to the thermal softening phenomenon, while the effect of temperature is only revealed on the thrust force when associated with the conditioning time. The hygrothermal factors (conditioning time in a humid environment and the conditioning temperature) have then the ability to modify the machining behavior by affecting the fiber shear and fiber spring-back due to the hydromechanical hardening and the hygrothermal damage on the interfaces as observed with both the SEM images and the machining forces.

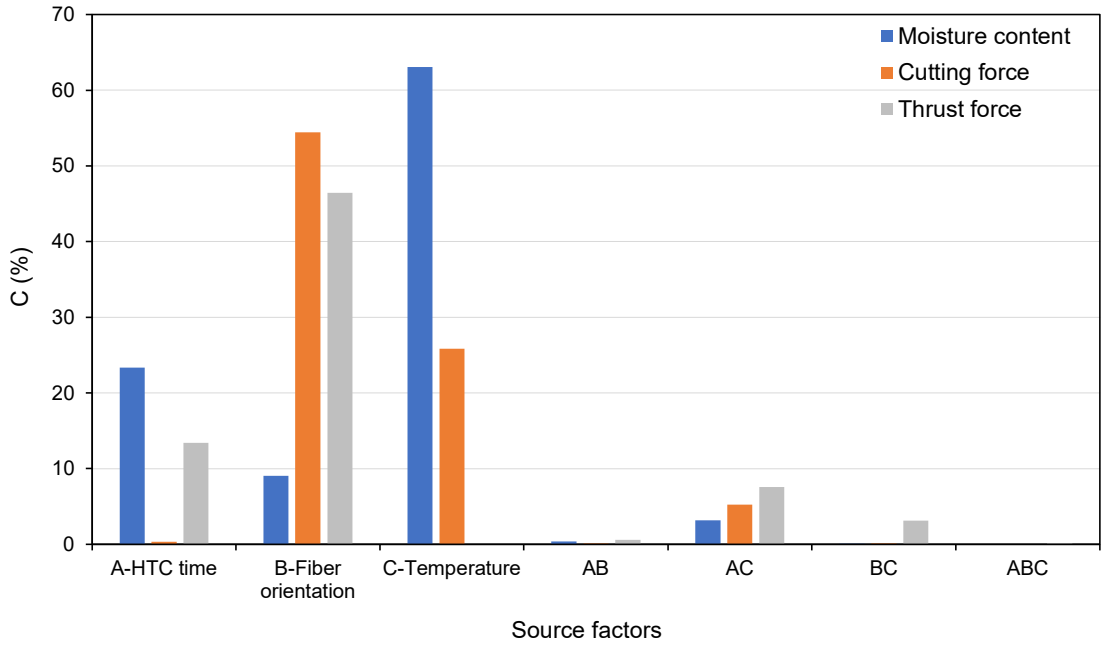


*Figure 14: Contribution rate of each input factor to the effect of water content, cutting force, and thrust force based on ANOVA*

## 4. Conclusions

This work aims to investigate the machining behavior of flax fiber-reinforced PLA biocomposites subjected to hygrothermal conditioning (HTC). The characterization of cutting behavior has been performed through the observation of the chip morphology, the evaluation of the machining forces, the assessment of the tool/chip interactions, and SEM analysis. This work leads to the following conclusions:

- The moisture diffusion in the biocomposite structure is accelerated when increasing the conditioning temperature. Moreover, increasing the fiber orientation regarding the sample length leads to an increase in the moisture content.
- The HTC effect on chip morphology is more important when flax fibers are oriented perpendicularly with respect to the feed direction. In this machining configuration, introducing HTC contributes to strong chip curling. Varying the HTC and/or the fiber orientation affects differently the bending moment to change the chip curvature radius by modifying the mechanical behavior of flax fibers and the polymer matrix.

- The tool/chip interaction is impacted by both the fiber orientation and the HTC times. These two factors lead to the change of the cutting behavior by introducing uncut fiber extremities and a high plastic flow of the polymer matrix. As a consequence, the presence of uncut fiber extremities on the tool/chip interface contributes to reducing friction, while the plastic flow of the polymer matrix induces an increase in the friction coefficient. These findings have been validated by the determination of the shear angle, the shear force, and the friction force using the analytical cutting model of Merchant. It has been shown via the analytical modeling that the increase of the fiber orientation from 45° to 90° under hygrothermal conditioning leads to changing the predominant cutting mechanism from friction to shear.
- Increasing the HTC time at 30°C enhances the cutting efficiency of flax fibers by hygrothermal hardening of the microfibrillar structure. After a long HTC time, the hygrothermal damage of the interfaces due to the hydrolysis process reduces the shearing efficiency of fibers and increases their transverse deformation, which induces important debonding zones on the machined surfaces.
- When increasing the conditioning temperature to 60°C, the thermal softening of the polymer matrix prevents an efficient shear of fibers. However, it contributes to reducing the debonding zones due to the increase of the thermomechanical plastic flow of the polymer matrix toward the cutting direction.
- The analysis of variance allows quantification of the contribution of each parameter and confirms that, in addition to the fiber orientation that determines the structural cutting configuration, cutting forces are more impacted by the conditioning temperature that controls the shear mechanism of flax fibers in the composite, while thrust forces are more influenced by the hygrothermal conditioning time because of

the fibers spring-back that is modified by the hygro-mechanical hardening of flax fibers.

## 5. References


[1] Akampumuza, O., Wambua, P. M., Ahmed, A., Li, W., and Qin, X.-H. H., 2017, "Review of the Applications of Biocomposites in the Automotive Industry," Polym. Compos., **38**(11), pp. 2553–2569.

[2] Soni, A., Kumar, S., Majumder, B., Dam, H., Dutta, V., and Das, P. K., 2023, "Synergy of Waste Plastics and Natural Fibers as Sustainable Composites for Structural Applications Concerning Circular Economy," Environ. Sci. Pollut. Res., pp. 1–20.

[3] Choudhary, S., Haloi, J., Sain, M. K., and Saraswat, P., 2023, "Advantages and Applications of Natural Fiber Reinforced Hybrid Polymer Composites in Automobiles: A Literature Review," *Lecture Notes in Mechanical Engineering*, Springer, Singapore, pp. 645–659.

[4] Akhil, U. V., Radhika, N., Saleh, B., Aravind Krishna, S., Noble, N., and Rajeshkumar, L., 2023, "A Comprehensive Review on Plant-Based Natural Fiber Reinforced Polymer Composites: Fabrication, Properties, and Applications," Polym. Compos., **44**(5), pp. 2598–2633.

[5] Shah, D. U., 2013, "Developing Plant Fibre Composites for Structural Applications by Optimising Composite Parameters: A Critical Review," J. Mater. Sci., **48**(18), pp. 6083–6107.

[6] "Bcomp Ltd. Switzerland" [Online]. Available: https://www.bcomp.ch/. [Accessed: 22-Jun-2023].

[7] Nassar, M. M. A., Arunachalam, R., and Alzebdeh, K. I., 2017, "Machinability of Natural Fiber Reinforced Composites: A Review," Int. J. Adv. Manuf. Technol., **88**(9–12), pp. 2985–3004.

[8] Chegdani, F., and Mansori, M. El, 2021, "Machining Behavior of Natural Fiber Composites," Encycl. Mater. Compos., **3**, pp. 168–185.

[9] Alarifi, I. M., 2023, "A Review on Factors Affecting Machinability and Properties of Fiber-Reinforced Polymer Composites," J. Nat. Fibers, **20**(1).

[10] Baley, C., and Bourmaud, A., 2021, "Multiscale Structure of Plant Fibers," Encycl. Mater. Compos., **3**, pp. 117–134.

[11] Chegdani, F., and El Mansori, M., 2019, "New Multiscale Approach for Machining Analysis of Natural Fiber Reinforced Bio-Composites," J. Manuf. Sci. Eng. Trans. ASME, **141**(1), p. 11004.

[12] Moudood, A., Rahman, A., Khanlou, H. M., Hall, W., Öchsner, A., and Francucci, G., 2019, "Environmental Effects on the Durability and the Mechanical Performance of Flax Fiber/Bio-Epoxy Composites," Compos. Part B Eng., **171**, pp. 284–293.

[13] Assarar, M., Scida, D., El Mahi, A., Poilâne, C., and Ayad, R., 2011, "Influence

of Water Ageing on Mechanical Properties and Damage Events of Two Reinforced Composite Materials: Flax-Fibres and Glass-Fibres," Mater. Des., **32**(2), pp. 788–795.

[14] Chilali, A., Zouari, W., Assarar, M., Kebir, H., and Ayad, R., 2018, "Effect of Water Ageing on the Load-Unload Cyclic Behaviour of Flax Fibre-Reinforced Thermoplastic and Thermosetting Composites," Compos. Struct., **183**(1), pp. 309–319.

[15] Placet, V., Cisse, O., and Boubakar, M. L., 2012, "Influence of Environmental Relative Humidity on the Tensile and Rotational Behaviour of Hemp Fibres," J. Mater. Sci., **47**(7), pp. 3435–3446.

[16] Stamboulis, A., Baillie, C. A., and Peijs, T., 2001, "Effects of Environmental Conditions on Mechanical and Physical Properties of Flax Fibers," Compos. Part A Appl. Sci. Manuf., **32**(8), pp. 1105–1115.

[17] Raj, S. S. R., Dhas, J. E. R., and Jesuthanam, C. P., 2021, "Challenges on Machining Characteristics of Natural Fiber-Reinforced Composites – A Review," J. Reinf. Plast. Compos., **40**(1–2), pp. 41–69.

[18] Baley, C., 2002, "Analysis of the Flax Fibres Tensile Behaviour and Analysis of the Tensile Stiffness Increase," Compos. - Part A Appl. Sci. Manuf., **33**(7), pp. 939–948.

[19] Chegdani, F., Takabi, B., El Mansori, M., Tai, B. L., and Bukkapatnam, S. T. S., 2020, "Effect of Flax Fiber Orientation on Machining Behavior and Surface Finish of Natural Fiber Reinforced Polymer Composites," J. Manuf. Process., **54**, pp. 337–346.

[20] Chegdani, F., Mezghani, S., and El Mansori, M., 2015, "Experimental Study of Coated Tools Effects in Dry Cutting of Natural Fiber Reinforced Plastics," Surf. Coatings Technol., **284**, pp. 264–272.

[21] Chegdani, F., and El Mansori, M., 2018, "Friction Scale Effect in Drilling Natural Fiber Composites," Tribol. Int., **119**, pp. 622–630.

[22] Chegdani, F., Mezghani, S., and El Mansori, M., 2016, "On the Multiscale Tribological Signatures of the Tool Helix Angle in Profile Milling of Woven Flax Fiber Composites," Tribol. Int., **100**, pp. 132–140.

[23] Chegdani, F., Takabi, B., Tai, B. L., Mansori, M. El, and Bukkapatnam, S. T. S., 2018, "Thermal Effects on Tribological Behavior in Machining Natural Fiber Composites," Procedia Manuf., **26**, pp. 305–316.

[24] Díaz-Álvarez, A., Díaz-Álvarez, J., Cantero, J. L., and Santiuste, C., 2020, "Analysis of Orthogonal Cutting of Biocomposites," Compos. Struct., **234**, p. 111734.

[25] Chegdani, F., and Mansori, M. El, 2018, "Mechanics of Material Removal When Cutting Natural Fiber Reinforced Thermoplastic Composites," Polym. Test., **67**, pp. 275–283.

[26] Chegdani, F., El Mansori, M., and Chebbi, A. A., 2021, "Cutting Behavior of Flax Fibers as Reinforcement of Biocomposite Structures Involving Multiscale Hygrometric Shear," Compos. Part B Eng., **211**, p. 108660.

[27] Regazzi, A., Corn, S., Ienny, P., Bénézet, J.-C. C., and Bergeret, A., 2016, "Reversible and Irreversible Changes in Physical and Mechanical Properties of Biocomposites during Hydrothermal Aging," Ind. Crops Prod., **84**, pp. 358–365.

[28] Scida, D., Assarar, M., Poilâne, C., and Ayad, R., 2013, "Influence of Hygrothermal Ageing on the Damage Mechanisms of Flax-Fibre Reinforced Epoxy Composite," Compos. Part B Eng., **48**, pp. 51–58.

[29] Li, Y., and Xue, B., 2016, "Hydrothermal Ageing Mechanisms of Unidirectional Flax Fabric Reinforced Epoxy Composites," Polym. Degrad. Stab., **126**, pp. 144–158.

[30] Thuault, A., Eve, S., Blond, D., Bréard, J., and Gomina, M., 2014, "Effects of the Hygrothermal Environment on the Mechanical Properties of Flax Fibres," J. Compos. Mater., **48**(14), pp. 1699–1707.

[31] Bos, H. L., Molenveld, K., Teunissen, W., van Wingerde, A. M., and van Delft, D. R. V, 2004, "Compressive Behaviour of Unidirectional Flax Fibre Reinforced Composites," J. Mater. Sci., **39**(6), pp. 2159–2168.

[32] Marrot, L., Lefeuvre, A., Pontoire, B., Bourmaud, A., and Baley, C., 2013, "Analysis of the Hemp Fiber Mechanical Properties and Their Scattering (Fedora 17)," Ind. Crops Prod., **51**, pp. 317–327.

[33] Chegdani, F., El Mansori, M., T. S. Bukkapatnam, S., and Reddy, J. N., 2019, "Micromechanical Modeling of the Machining Behavior of Natural Fiber-Reinforced Polymer Composites," Int. J. Adv. Manuf. Technol., **105**(1–4), pp. 1549–1561.

[34] Omodara, O., Daramola, O. O., Olajide, J. L., Adediran, A. A., Akintayo, O. S., Adewuyi, B. O., Desai, D. A., and Sadiku, E. R., 2020, "Improved Mechanical and Wear Characteristics of Hypereutectic Aluminium-Silicon Alloy Matrix Composites and Empirical Modelling of the Wear Response," Cogent Eng., **7**(1).

[35] Chegdani, F., Mezghani, S., and El Mansori, M., 2017, "Correlation between Mechanical Scales and Analysis Scales of Topographic Signals under Milling Process of Natural Fibre Composites," J. Compos. Mater., **51**(19), pp. 2743–2756.

[36] Abena, A., Soo, S. L., Ataya, S., Hassanin, H., El-Sayed, M. A., Ahmadein, M., Alsaleh, N. A., Ahmed, M. M. Z., and Essa, K., 2023, "Chip Formation and Orthogonal Cutting Optimisation of Unidirectional Carbon Fibre Composites," Polymers (Basel)., **15**(8), p. 1897.

[37] Calzada, K. A., Kapoor, S. G., Devor, R. E., Samuel, J., and Srivastava, A. K., 2012, "Modeling and Interpretation of Fiber Orientation-Based Failure Mechanisms in Machining of Carbon Fiber-Reinforced Polymer Composites," J. Manuf. Process., **14**(2), pp. 141–149.

[38] Li, H., Qin, X., He, G., Jin, Y., Sun, D., and Price, M., 2016, "Investigation of Chip Formation and Fracture Toughness in Orthogonal Cutting of UD-CFRP," Int. J. Adv. Manuf. Technol., **82**(5–8), pp. 1079–1088.

[39] Cook, N. H., Jhaveri, P., and Nayak, N., 1963, "The Mechanism of Chip Curl and Its Importance in Metal Cutting," J. Manuf. Sci. Eng. Trans. ASME, **85**(4), pp. 374–380.

[40] Liu, P. D., Hu, R. S., Zhang, H. T., and Wu, X. S., 1992, "A Study on Chip Curling and Breaking," *Proceedings of the Twenty-Ninth International Matador Conference*, J. Atkinson, G. Barrow, M. Burdekin, N.R. Chitkara, and R.G. Hannam, eds., Macmillan Education UK, London, pp. 507–512.

[41] Van Schoors, L., Cadu, T., Moscardelli, S., Divet, L., Fontaine, S., and Sicot, O., 2021, "Why Cyclic Hygrothermal Ageing Modifies the Transverse Mechanical Properties of a Unidirectional Epoxy-Flax Fibres Composite?," Ind. Crops Prod., **164**, p. 113341.

[42] Le Duigou, A., and Castro, M., 2017, "Hygromorph BioComposites: Effect of Fibre Content and Interfacial Strength on the Actuation Performances," Ind. Crops Prod., **99**, pp. 142–149.

[43] Le Duigou, A., and Castro, M., 2015, "Moisture-Induced Self-Shaping Flax-Reinforced Polypropylene Biocomposite Actuator," Ind. Crops Prod., **71**, pp. 1–6.

[44] Nguyen, H. T. H., Qi, P., Rostagno, M., Feteha, A., and Miller, S. A., 2018, "The Quest for High Glass Transition Temperature Bioplastics," J. Mater. Chem. A, **6**(20), pp. 9298–9331.

[45] Kim, K. S., Ando, Y., and Kim, K. W., 2008, "The Effect of Temperature on the Nanoscale Adhesion and Friction Behaviors of Thermoplastic Polymer Films," Nanotechnology, **19**(10), p. 105701.

[46] Nirmal, U., Low, K. O., and Hashim, J., 2012, "On the Effect of Abrasiveness to Process Equipment Using Betelnut and Glass Fibres Reinforced Polyester Composites," Wear, **290**–**291**, pp. 32–40.

[47] Yousif, B. F., and El-Tayeb, N. S. M., 2008, "Adhesive Wear Performance of T-OPRP and UT-OPRP Composites," Tribol. Lett., **32**(3), pp. 199–208.

[48] Nirmal, U., Hashim, J., and Low, K. O., 2012, "Adhesive Wear and Frictional Performance of Bamboo Fibres Reinforced Epoxy Composite," Tribol. Int., **47**, pp. 122–133.

[49] Burgert, I., and Fratzl, P., 2009, "Plants Control the Properties and Actuation of Their Organs through the Orientation of Cellulose Fibrils in Their Cell Walls," Integr. Comp. Biol., **49**(1), pp. 69–79.

[50] Eugene Merchant, M., 1944, "Basic Mechanics of the Metal-Cutting Process," J. Appl. Mech. Trans. ASME, **11**(3), pp. A168–A175.

[51] Brown, C. A., 2001, "Machining of Metals: Fundamentals," Encycl. Mater. Sci. Technol., pp. 4703–4708.